

Field-induced cation migration in Cu oxide films by *in situ* scanning tunneling microscopy

J. P. Singh,^{a)} T.-M. Lu, and G.-C. Wang

Department of Physics, Applied Physics and Astronomy, Rensselaer Polytechnic Institute, Troy, New York 12180-3590

(Received 27 December 2002; accepted 23 April 2003)

We observed the formation of Cu metallic nanoscale structures of ~ 20 -nm diameter and ~ 2 -nm height on a Cu_2O covered polycrystalline Cu film under an applied field using a scanning tunneling microscope tip in a high vacuum condition. We interpreted the results as the Cu cation transport through the copper oxide film towards the surface when a positive biased voltage (>1.5 V) was applied to the film to lower the activation energy of the cation migration. Scanning tunneling spectroscopy measurements showed that the field-induced nanostructures were pure metallic Cu with a characteristic broad peak near -0.45 eV. No structural change was observed when a negative bias was applied to the film. © 2003 American Institute of Physics. [DOI: 10.1063/1.1586461]

The scanning tunneling microscopy (STM) has been used intensively for imaging metal and semiconductor surfaces in the last two decades. In addition to revealing surface morphologies and electronic structures with a spatial resolution of a few angstroms, STM has also been successfully applied for the fabrication of nanostructures and manipulating atoms on surfaces.¹⁻¹³ Recently, STM has also been shown to be capable of controlling ion migration in dielectrics.¹⁴ In a very interesting study of STM-induced void formation at the $\text{Al}_2\text{O}_3/\text{Ni}_3\text{Al}$ interface, the interfacial Al metal atoms were found to be oxidized via transport into the oxide, and Al cations in the oxide layer rapidly diffused away.¹⁴ Field-induced ion migration is of particular interest in Cu technology since Cu is now used in advanced integrated circuitry. Cu ion migration may cause a reliability problem when placed in a dielectric containing oxygen.¹⁵

In this letter, we report a phenomenon of localized mass transport induced by the electric field of a STM tip in a high vacuum condition on a polycrystalline Cu thin film that was air-exposed and had a layer of copper oxide on the surface. We observed the formation of a nanoscale metallic structure over the Cu oxide film surface for the sample bias voltage higher than a threshold voltage of 1.5 V. If the polarity of the bias voltage was reversed, no nanostructure was formed. The driving force for the mass transport is interpreted as the reduction of the local potential energy barrier to cation diffusion at the $\text{Cu}_2\text{O}/\text{Cu}$ interface.

A ~ 17 -nm-thick polycrystalline Cu film was grown on a *n*-Si (resistivity $1 \Omega \text{ cm}$) substrate by thermal evaporation with a rate of 0.10 ± 0.05 nm/min in a UHV chamber with a base pressure of 4×10^{-10} Torr.¹⁶ The Si substrate was cleaned by the RCA method and a thin oxide layer was grown on the Si surface. The Cu film was taken out from the deposition chamber and kept in the atmosphere for one week for oxidation. The formation of an oxide layer on Cu thin film was examined by x-ray photoelectron spectroscopy (XPS) in another UHV chamber. $\text{Cu } 2p_{3/2}$ and $\text{Cu } 2p_{1/2}$ peaks were observed at 932.9 and 952.7 eV, respectively, from the XPS spectrum shown in Fig. 1. The absence of

satellite peaks of $\text{Cu } 2p_{3/2}$ and $\text{Cu } 2p_{1/2}$ is an indication of the existence of a Cu_2O layer. This is consistent with the previous studies that copper oxide formed at room temperature in air consists of copper (I) oxide, Cu_2O .¹⁷⁻¹⁹ The Cu and Cu_2O have a very close binding energy, with a difference of 0.1 eV, and cannot be resolved in our XPS spectrum. However, these peaks can be seen from the LMM Auger transitions shown in the inset in Fig. 1. Although we cannot determine the oxide thickness from the XPS spectrum, we estimate the thickness to be ~ 5 nm based on the inverse logarithmic growth law of copper oxide for a one-week exposure in the atmosphere.²⁰

The surface morphology was imaged by a homemade STM system.²¹ The tip used was Pt-Ir for its resistance against oxidation. All the STM measurements were performed in a vacuum chamber with a pressure better than 3×10^{-9} Torr. All the images are 256×256 pixels with a

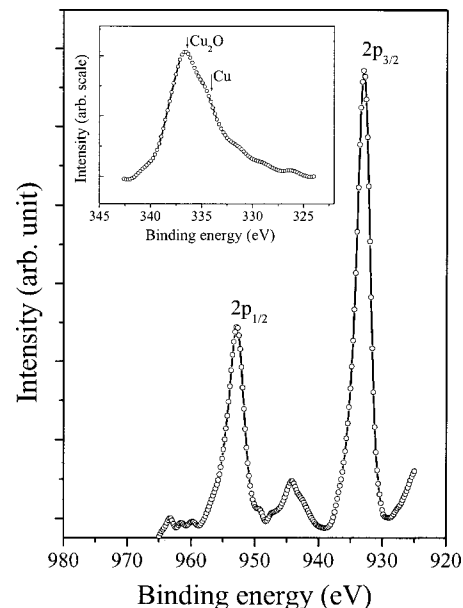


FIG. 1. X-ray photoelectron spectroscopy spectrum showing $\text{Cu } 2p_{3/2}$ peak at 932.9 eV and $\text{Cu } 2p_{1/2}$ at 952.7 eV from ~ 17 -nm-thick copper film grown by thermal evaporation in a UHV condition and then air exposed for oxidation. The inset shows Auger LMM transitions of Cu and Cu_2O peaks.

^{a)}Electronic mail: singhj@rpi.edu

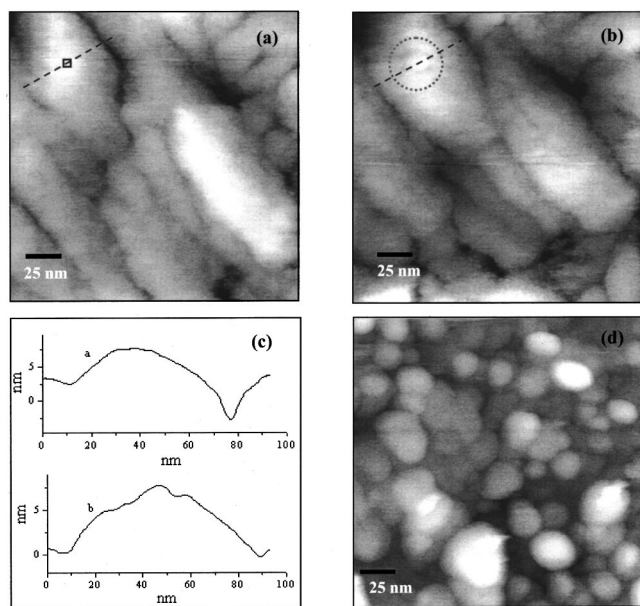


FIG. 2. (a) STM image of Cu film under constant current of ~ 1 nA and sample bias voltage of 0.2 V for a control sample surface, (b) after the Cu film was biased at 2 V at a fixed position labeled by the square in (a) for 2 min, (c) line scans before and after the formation of a nanoisland along the dashed lines in Figs. 2(a) and 2(b), (d) general change in the morphology after the film was biased at 2 V and scanned over the entire 200×200 nm² area.

10-ms time interval between pixels for data acquisition. A STM image of the air-exposed Cu film surface using a nominal bias of 0.2 V to sample and constant tunneling current of ~ 1 nA is shown in Fig. 2(a). The surface topography shows randomly oriented island structures of nonuniform sizes.

During the scanning of the surface at elevated bias (positive) voltages, the feedback pulls the tip away from the surface slightly to compensate for the higher voltage. A rise of the electric field strength can be expected as the current depends exponentially on the distance, but only linearly on the voltage.²² Therefore, any surface modification expected using this procedure is due to the higher electric field (or voltage) because the current remains unchanged. Figure 2(b) shows a nanoisland of ~ 20 nm (labeled by the dashed circle) created after the tip was stationed at the position labeled by the square in Fig. 2(a) for 2 min at a 2 V bias applied to the sample. At the tip-surface distance of 1 nm and bias voltage of 2 V, the electric field strength is estimated to be 20 MV/cm. The surface topographical changes were detected by *in situ* scanning the same area under the normal constant current mode with a feedback loop set at 1 nA and a 0.2 V bias voltage. Figure 2(c) shows the line scans over the Cu oxide surface before [Fig. 2(a)] and after [Fig. 2(b)] the development of the nanoisland. It is important to note that in the process of the development of a nanoisland on the Cu oxide surface, there are considerable morphological changes occurring in regions well outside the nanoisland. Figure 2(d) shows an image taken after scanning the entire 200×200 -nm² area at the same elevated bias voltage of 2 V. Significant topographical changes showing nanoscale structures are visible all over the scanned surface area. The nanostructures have an average diameter of 20 ± 5 nm and an average height of ~ 2 nm. In all these experiments, the sample surface was positively biased and the electrons flowed from

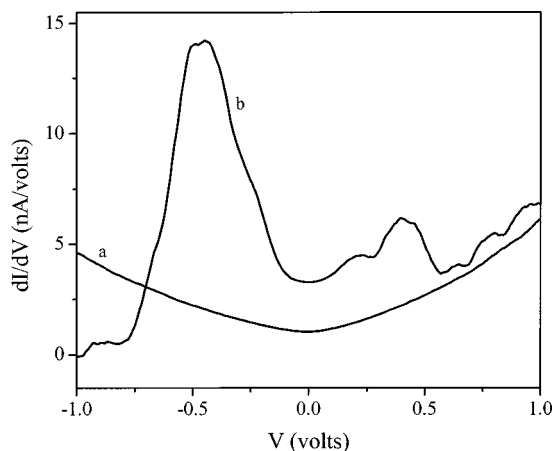


FIG. 3. The dI/dV spectra of (a) the Cu oxide surface and (b) nanoisland obtained after applying a 2 V bias voltage on the Cu oxide covered film. The peak near -0.45 V is a characteristic of metallic Cu surface state and was consistently observed from each of the ten different freshly formed nanoislands on the Cu oxide surface. Whereas, no such peak was visible in all the dI/dV spectra of Cu oxide.

the tip to the surface. When an elevated reverse bias (-2 V) was applied to the sample surface (electrons flowed from the sample to the tip), no nanostructure was formed and the surface remained similar to the control surface image shown in Fig. 2(a).

Scanning tunneling spectroscopy (STS) spectra collected from the original Cu oxide surface and the freshly formed nanoisland shown in Fig. 2(b) are shown in Fig. 3. The STS measurements were taken at ten different positions on Cu oxide surface and at ten different freshly formed nanoislands. Over 20 dI/dV spectra measured at one position were averaged and plotted. The average removed the random noises and not the characteristic feature such as the peak at -0.45 eV for nanoislands in curve (b). Spectra taken at different positions on Cu oxide surface look similar to curve (a). The broad peak near -0.45 V in Fig. 3(b) is consistent with the broad surface state peak observed from a pure Cu crystal at -0.4 eV below the Fermi level by STS and ultraviolet photoelectron emission reported in the literature.^{23,24} No such peak was observed from the original Cu oxide surface, as shown in Fig. 3(a).

The observed field-induced Cu nanostructures are not related to the conventional electromigration damage in Cu films, where the atom migration takes place in the direction of the electron-wind.^{25,26} It is also not due to the field-induced electromigration inside the metallic Cu film, where the electric field is small. If either case were true, the reverse polarity would generate holes at the sample surface, which was not observed in our experiment. Our Cu thin film was oxidized in air to form a Cu₂O layer on the top of the surface. Cu ionic transport in the Cu₂O film can occur under a sufficiently large field and the cation vacancy migration takes place simultaneously. The schematic diagram in Fig. 4 shows the effect of tip-induced electric field E on the cation injection at the Cu₂O/Cu interface and cation migration in the oxide. The high electric field between the tip and the film is expected to lower the potential barrier for the cation at the Cu₂O/Cu interface, to enhance the cation injection, and to increase the cation migration towards the Cu₂O/vacuum interface. This will, in turn, enhance the cation vacancy migra-

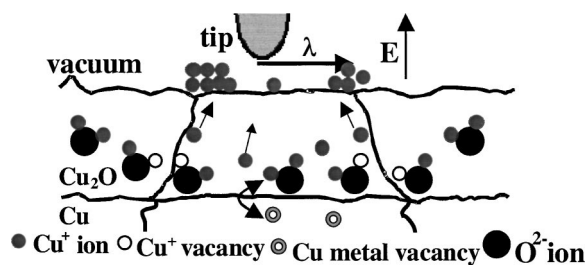


FIG. 4. A schematic showing the Cu ion transport across the Cu_2O layer under the positive bias applied to the Cu film under the electric field of an STM tip. Two grain boundaries are also shown in the oxide layer.

tion within the oxide layer. The activation energy of cation migration in oxide is lowered by $1/2qaE$, where q is the charge of the carrier, a is the jump distance, and E is the field strength.^{18,27} The barrier height for cation injection into the oxide is also lowered. The process of field-enhanced metal ion injection into the oxide and field-enhanced cation migration continues as long as the field is present.

For the high electric field near the STM tip, the electrons produce a charge region (spreading resistance region) near the surface, which extends to about the length of the electron mean free path λ .²⁸ If we assume the charge region near the point of closest tip-sample distance has a spherical symmetry with a radius λ , then the lowering of the potential barrier by the electric field of STM tip occurs locally in that zone. Note that the thickness of the oxide film ~ 5 nm is less than the charge region $\sim \lambda$ ($= 40$ nm).²⁹ Under the electric field, the mass transport continues until the field is shielded by the newly formed pure Cu island. The newly formed Cu island would stay metallic-like because the chamber has a high vacuum environment. This allows us to measure the pure Cu surface states using the STS technique (see Fig. 3).

The field-induced Cu migration tends to form small islands, as shown in Fig. 2(d), instead of a uniform layer of Cu. Each large Cu island in the control surface [Fig. 2(a)] actually consists of many small grains with many grain boundaries (GBs) in a higher-resolution image (not shown in the current figure). The presence of GBs provides an easy path for the defect migration. The actual size of the nanoscale structures will certainly depend on the details of the microstructure of the film such as GBs, grain orientation, and grain size distributions in addition to the time that the positive bias was applied to the sample. The histograms of the field-induced size distribution of the nanoscale structures at varying bias voltages showed a gamma distribution. The average size of the nanostructures (~ 20 nm) and its size distribution does not seem to change with the bias voltage (1.5 to 2.5 V) within the finite statistics of sampling. After the islands are grown to the ~ 20 -nm size, the metallic-like islands serve as a shield to prevent the penetration of the electric field into the oxide and thereby stop the island growth.

Field-induced ionic penetration in dielectric film is an extremely important issue in advanced integrated circuit fabrication, especially when Cu is used. It is interesting to compare our present work with a recent experiment of Cu ionic diffusion in an oxygen-containing dielectric film using a technique called bias temperature stress measurement, where an electric field (on the order of 1 MV/cm) was applied to the metal-dielectric-semiconductor (MIS) structure.¹⁵ In that

case, the Cu electrode was deposited onto the dielectric surface and the Cu atoms at the Cu/dielectric interface therefore inevitably got oxidized. When a strong positive electric field was applied to the electrode, Cu ions were ejected from the Cu/Cu oxide interface and migrated to the dielectric/Si interface. The Cu charge density at the dielectric/Si interface was then detected indirectly by measuring the changes in the capacitance characteristics of the MIS sample. In this analogy, our present STM measurement of the Cu ion migration in the Cu oxide film under a strong electric field is a more direct measurement of the phenomenon.

In summary, we have shown the formation of the metallic nanoscale structures on an oxidized Cu film surface as a result of the local mass transport induced by the electric field in the Cu oxide film by using an STM tip. These results are fundamentally different from the field-induced evaporation and surface diffusion, local surface melting, and Taylor cone formation reported in the literature, as well as the conventional electromigration damage in Cu films.

The work was supported by NSF and SRC. We thank Jason Drotar for growing the Cu film and Fu Tang for taking XPS. Special thanks go to Paul Ho for insightful comments.

- ¹H. J. Mamin, S. Chiang, H. Birk, P. H. Guethner, and D. Rugar, *J. Vac. Sci. Technol. B* **9**, 1398 (1991).
- ²H. J. Mamin, P. H. Guethner, and D. Rugar, *Phys. Rev. Lett.* **65**, 2418 (1990).
- ³G. S. Hsiao, R. M. Penner, and J. Kingsley, *Appl. Phys. Lett.* **64**, 1350 (1994).
- ⁴Z. L. Ma, N. Liu, W. B. Zhao, Q. J. Gu, X. Ge, Z. Q. Xue, and S. J. Pang, *J. Vac. Sci. Technol. B* **13**, 1212 (1995).
- ⁵J. A. Stroscio and D. M. Egler, *Science* **254**, 1319 (1991).
- ⁶C. T. Salling and M. G. Lagally, *Science* **265**, 502 (1994).
- ⁷J. Rabe and S. Buchholz, *Appl. Phys. Lett.* **58**, 702 (1991).
- ⁸S. E. McBride and G. C. Wetsel, *Appl. Phys. Lett.* **59**, 3056 (1991).
- ⁹A. A. Shklyae, M. Shibata, and M. Ichikawa, *J. Vac. Sci. Technol. B* **18**, 2339 (2000).
- ¹⁰D. M. Egler, C. P. Lutz, and W. E. Rudge, *Nature (London)* **352**, 600 (1991).
- ¹¹T. T. Tsong, *Phys. Rev. B* **44**, 13703 (1991).
- ¹²U. Staufer, R. Wiesendanger, L. Eng, L. Rosenthaler, H. R. Hidber, H.-J. Güntherodt, and N. García, *Appl. Phys. Lett.* **51**, 244 (1987).
- ¹³P. F. Marella and R. F. Pease, *Appl. Phys. Lett.* **55**, 2366 (1989).
- ¹⁴N. P. Magtoto, C. Niu, M. Anzaldúa, J. A. Kelber, and D. R. Jennison, *Surf. Sci.* **L157**, 472 (2001).
- ¹⁵A. Mallikarjunan, S. P. Murarka, and T.-M. Lu, *Appl. Phys. Lett.* **79**, 1855 (2001).
- ¹⁶J. T. Drotar, Ph.D. thesis, Rensselaer Polytechnic Institute, Troy, NY, 2002.
- ¹⁷C. H. Yoon and D. L. Cocke, *J. Electrochem. Soc.* **134**, 643 (1987).
- ¹⁸D. L. Cocke, G. K. Chuah, N. Kruse, and J. H. Block, *Appl. Surf. Sci.* **84**, 153 (1995).
- ¹⁹Y. S. Chu, I. K. Robinson, and A. A. Gewirth, *J. Chem. Phys.* **110**, 5952 (1999).
- ²⁰J. C. Yang, B. Kolasa, J. M. Gibson, and M. Yeadon, *Appl. Phys. Lett.* **73**, 2841 (1998).
- ²¹A. Chan, Ph.D. thesis, Rensselaer Polytechnic Institute, Troy, NY, 1996.
- ²²Ch. Mascher and B. Damaschke, *J. Appl. Phys.* **75**, 5438 (1994).
- ²³A. L. V. Parga, F. J. García-Vidal, and R. Miranda, *Phys. Rev. Lett.* **85**, 4365 (2000).
- ²⁴O. Sánchez, J. M. García, P. Segovia, J. Alvarez, A. L. V. Parga, J. E. Ortega, M. Prietsch, and R. Miranda, *Phys. Rev. B* **52**, 7894 (1995).
- ²⁵P. S. Ho and T. Kwok, *Rep. Prog. Phys.* **52**, 301 (1989).
- ²⁶*Diffusion Phenomenon in Thin Films and Microelectronic Materials*, edited by D. Gupta and P. S. Ho (Noyes, New York, 1988).
- ²⁷A. Atkinson, *Rev. Mod. Phys.* **57**, 437 (1985).
- ²⁸F. Flores and N. García, *Phys. Rev. B* **30**, 2289 (1984).
- ²⁹F. Chen and D. Gardner, *IEEE Electron Device Lett.* **19**, 508 (1998).